Three-dimensional numerical study of mixed convection within a ventilated cavity (Shape ' L ') crossed by a nanofluid under the effect of a magnetic field

S. KHERROUBI, K. RAGUI, N. LABSI, Y.K. BENKAHLA AND A. BOUTRA*

Laboratory of Transport Phenomena. USTHB. Algiers. Algeria.
(BP. 32 El Alia, 16111 Bab Ezzouar, Algiers, Algeria)
**Corresponding author: Tel: +213 05 60 44 40 09 Email: sddikr@yahoo.fr*

Abstract The present work is dedicated to the three-dimensional numerical study of mixed convection heat transfer, taking place within a ventilated cavity (of shape L) crossed by Cu-water nanofluid. The enclosure is subjected to the action of a magnetic field. The ventilation is assured by two openings of the same size. The cold flow enters by an opening practiced at the top of the left wall, and exits by another opening practiced at the bottom of the right vertical wall. All the cavity walls are maintained at the same temperature, superior to that of the entering flow, except the side walls which are considered as adiabatic. The control parameters are: the Reynolds number and the Hartmann number as well as the nanoparticles volume fraction.

NOMENCLATURE

B_0	External magnetic field	T
Cp	Constant pressure specific heat	J $kg^{-1}.K^{-1}$
F	Lorentz force	N m^{-3}
G	Gravitational acceleration	m s^{-2}
H	Height of cavity	m
Ha	Hartman number	
L	Length of the cavity	m
Nu	Nusselt number	
p	Pressure	Pa
P	Dimensionless pressure	
Pr	Number	
Re	Reynolds number	
Ri	Richardson number	
T	Temperature	K
(x, z ,y)	Cartesian coordinates	m
(u, w, v)	Velocity components in the x-, z- and y-directions	m s^{-1}

Greek symbols

α	Thermal diffusivity	m^2 s^{-1}
β	Thermal expansion coefficient	K^{-1}
ρ	Density	Kg m^{-3}
ν	Kinematic viscosity	m^2 s^{-1}
μ	Dynamic viscosity	Kg m^{-1} s^{-1}
θ	Dimensionless temperature	
φ	Particle volume fraction	
σ	Electrical conductivity	$(\Omega m)^{-1}$

Superscript

Avg	Average
bf	base fluid
nf	Nanofluid
n	Normal direction to the considered wall.
s	Solid particles

INTRODUCTION

Mixed convection heat transfer in vented cavities has a wide variety of technological applications such as cooling of electronic device, solar collector, home ventilation and etc [1]. In recent years, mixed convection inside various shaped cavities enclosures with nanofluids has attracted attention in variety of engineering applications. Mahmud et al. [2] and Tasnim et al. [3] about natural convection inside air filled L-shaped cavities, Mahmud et al. [4] study free convection in arc shaped cavities and Koca et al. [5] study same problem within triangular cavities. The study of MHD flow in these cavities has gained much attraction of researchers due to the effect of magnetic field on the flow control. Sheikholeslami et al. [6] studied the MHD nanofluid flow in a double-sided lid-driven wavy cavity. Chamkha and al. [7-14] have analyzed the use of various types and models of nanofluids in different geometries including single and double lid-driven cavities. Ghasemi et al. [15], Mahmoudi et al. [16] and Ghasemi [17] examined the effects of nanofluids and magnetic field on natural convection in square, triangular and U-shaped cavities, respectively, in which they denoted that, the magnetic field resulted in the decrease of convective cell flow within the enclosures and as a result a reduction of heat transfer rate. They also argued that, the use of nanofluids could enhance the heat transfer rate. Moreover the thermal

Corresponding author: sddikr@yahoo.fr

© The Authors, published by EDP Sciences. This is an open access article distributed under the terms of the Creative Commons Attribution License 4.0 (http://creativecommons.org/licenses/by/4.0/).

performance of the enclosure was found to be a function of the enclosure aspect ratio. In addition, H. M. Elshehabey et al. [18] studied the natural convection in an inclined L-shaped enclosure filled with Cu-water nanofluid with differentially heated walls in the presence of an inclined magnetic field. It was found that, the presence of the magnetic field in the fluid region causes a significant reduction in the fluid flow and heat transfer characteristics. Also, a good enhancement in the heat transfer rate can be obtained by adding the copper nanoparticles to the pure fluid.

From this brief literature review, we find that the majority of investigations examining the 2D model of nanofluid flow within different geometries. However, the flow of nanofluids in the L-shaped cubic cavity in the presence of a magnetic field has not yet been reported in the literature. So, in this work, the problem of the mixed convection of Cu-water nanofluid inside an L-shaped cubic cavity is numerically studied. The effects of Reynolds number, Hartmann number and volume fraction of Cu nanoparticles on fluid characteristics and temperature field are considered.

MATHEMATICAL FORMULATION

The geometry of the ventilated L-shaped cubic cavity with the dimensions is shown in Fig. 1, the Cu-water (Pr = 5) nanofluid is passed through the cubic cavity by two openings of the same size (0.15 H) practiced on the vertical walls under the presence of the vertical magnetic field .The cold nanofluid enters the cavity into opening located at the left vertical wall and exits through the opening located at the right wall. All walls of the cubic cavity are hot except the side walls are considered adiabatic. The thermophysical properties of Water and Copper nanoparticle are given in Table 1. [19]

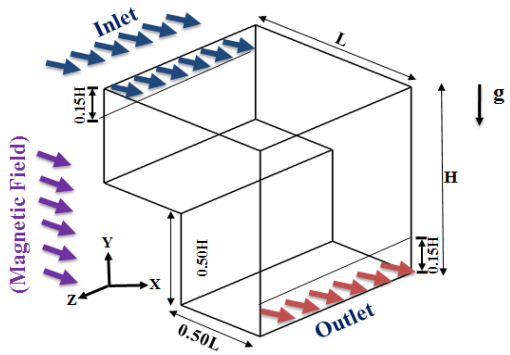

Fig.1 Physical problem

The following assumptions have been made:

(a) The base fluid (water) and the solid spherical nanoparticles (Cu) are in thermal equilibrium.

(b) The flow is considered to be steady, three-dimensional and laminar.

(c) The nanofluid is Newtonian and incompressible.

(e) Boussinesq approximation is used to determine the variation of density in the buoyancy term where the other thermophysical properties of the nanofluid are assumed constant.

(f) The radiation, dissipation and joule heating effects are negligible.

(g) The uniform magnetic field with a constant magnitude **(B)** is applied vertically. The induced magnetic field assumed to be negligible in comparison with the external magnetic field. Moreover, the imposed and induced electrical fields are assumed to be negligible. Consequently, the electric current density and the Lorentz forces are reduced to $\left(\vec{J}=\sigma_{nf}\left(\vec{V}\wedge\vec{B}\right)\right)$ and $\left(\vec{F}=\left(\vec{J}\wedge\vec{B}\right)\right)$, respectively.

Table 1
Thermophysical properties of the base fluid and the Cu nanoparticles [**19**].

	Cp (J kg^{-1} K^{-1})	ρ (kg.m^{-3})	K (W m^{-1} K^{-1})	β (K^{-1})
Water	4179	997,1	0,613	21×10^{5}
Cu	385	8933	401	1.67×10^{5}

The set of non-dimensional term used in our analysis are as follows;

$$\theta=\frac{T-T_{Inlet}}{T_{Wall}-T_{Inlet}} \qquad P=\frac{p}{\rho_{nf}u_{Inlet}^{2}} \qquad Pr=\frac{\nu_{bf}}{\alpha_{bf}}$$

$$Re=\frac{u_{Inlet}H}{\nu_{bf}} \qquad Ha=B_0 L\left(\frac{\sigma_{nf}}{\mu_{bf}}\right)^{1/2} \qquad \alpha_{nf}=\frac{k_{nf}}{(\rho Cp)_{nf}}$$

$$(U,V,W)=\frac{(u,v,w)}{u_{Inlet}} \qquad (1)$$

The mass density, the heat capacitance and the thermal expansion coefficient of the nanofluid are [29]:

$$\rho_{nf}=(1-\varphi)\rho_{bf}+\varphi\rho_{s} \qquad (2)$$

$$(\rho Cp)_{nf}=(1-\varphi)(\rho Cp)_{bf}+\varphi(\rho Cp)_{s} \qquad (3)$$

$$(\rho\beta)_{nf}=(1-\varphi)(\rho\beta)_{bf}+\varphi(\rho\beta)_{s} \qquad (4)$$

The effective dynamic viscosity of the nanofluid is given by Brinkman [20].

$$\frac{\mu_{nf}}{\mu_{bf}}=(1-\varphi)^{-2.5} \qquad (5)$$

The thermal conductivity of the nanofluid k_{nf} was given by Maxwell [21]

$$\frac{k_{nf}}{k_{bf}}=\frac{(k_s+2k_{bf})-2\varphi(k_{bf}-k_s)}{(k_s+2k_{bf})+\varphi(k_{bf}-k_s)} \qquad (6)$$

Under the assumptions and the non-dimensional variables above, the dimensionless transport equations for mass, momentum and thermal energy are:

$$\frac{\partial U}{\partial X}+\frac{\partial V}{\partial Y}+\frac{\partial W}{\partial Z}=0 \qquad (7)$$

$$U\frac{\partial U}{\partial X}+V\frac{\partial U}{\partial Y}+W\frac{\partial U}{\partial Z}=-\frac{\partial P}{\partial X}+\frac{\mu_{nf}}{\rho_{nf}\nu_{bf}}\frac{1}{Re_{bf}}\left(\frac{\partial^2 U}{\partial X^2}+\frac{\partial^2 U}{\partial Y^2}+\frac{\partial^2 U}{\partial Z^2}\right)-\frac{\rho_{bf}}{\rho_{nf}}\frac{Ha^2}{Re_{bf}}U \qquad (8)$$

Corresponding author: sddikr@yahoo.fr

$$U\frac{\partial V}{\partial X}+V\frac{\partial V}{\partial Y}+W\frac{\partial V}{\partial Z}=-\frac{\partial P}{\partial Y}+\frac{\mu_{nf}}{\rho_{nf}\nu_{bf}}\frac{1}{Re_{bf}}\left(\frac{\partial^2 V}{\partial X^2}+\frac{\partial^2 V}{\partial Y^2}+\frac{\partial^2 V}{\partial Z^2}\right)+\frac{(\rho\beta)_{nf}}{\rho_{nf}\beta_{bf}}Ri\,\theta \quad (9)$$

$$U\frac{\partial W}{\partial X}+V\frac{\partial W}{\partial Y}+W\frac{\partial W}{\partial Z}=-\frac{\partial P}{\partial Z}+\frac{\mu_{nf}}{\rho_{nf}\nu_{bf}}\frac{1}{Re_{bf}}\left(\frac{\partial^2 W}{\partial X^2}+\frac{\partial^2 W}{\partial Y^2}+\frac{\partial^2 W}{\partial Z^2}\right)-\frac{\rho_{bf}}{\rho_{nf}}\frac{Ha^2}{Re_{bf}}W \quad (10)$$

$$U\frac{\partial \theta}{\partial X}+V\frac{\partial \theta}{\partial Y}+W\frac{\partial \theta}{\partial Z}=\frac{\alpha_{nf}}{\alpha_{bf}}\frac{1}{Re_{bf}\,Pr}\left(\frac{\partial^2 \theta}{\partial X^2}+\frac{\partial^2 \theta}{\partial Y^2}+\frac{\partial^2 \theta}{\partial Z^2}\right) \quad (11)$$

The velocity and temperature boundary conditions are expressed as:

- Hot walls: U= V= W= 0 and θ = 1;
- Inlet port: U= 1, V= W= 0 and θ = 0
- Outlet port: ∂U/∂X= ∂V/∂X= ∂W/∂X = 0 and ∂θ/∂X = 0;
- On the side walls: adiabatic walls.

The total average Nusselt number is obtained by integrating the local Nusselt number along the hot walls as follows:

$$Nu_{Local}=-\frac{k_{nf}}{k_{bf}}\frac{\partial \theta}{\partial n}\bigg|_{Wall} \quad (12)$$

$$Nu_{Avg}=\frac{1}{4}\sum\left(\begin{array}{l}\int_0^1\int_{0.5}^{0.85}Nu\big|_{X=0}\,dY\,dZ+\int_0^1\int_0^{0.5}Nu\big|_{X=0.5}\,dY\,dZ\\+\int_0^1\int_0^1 Nu\big|_{X=1}\,dY\,dZ+\int_0^1\int_0^1 Nu\big|_{Z=1}\,dX\,dY\\+\int_0^{0.5}\int_0^1 Nu\big|_{Z=0}\,dX\,dY+\int_{0.5}^1\int_0^1 Nu\big|_{Z=0}\,dX\,dY\end{array}\right) \quad (13)$$

NUMERICAL METHOD AND VALIDATION

The governing equations associated with the boundary conditions have been solved iteratively by the finite volume method given by Patankar [22]. The SIMPLER algorithm has been adopted for pressure-velocity coupling calculations. The algebraic system resulting from digital discretization was calculated using TDMA. Iteration in the code is stopped when the convergence residual is greater than 10^{-6}.

In order to validate the numerical code, natural convection in an L-shaped 2D cavity filled with air for aspect ratio equal to 0.25 is analyzed. The results are compared with existing results in the literature. For different Rayleigh numbers, the average Nusselt numbers are compared with those of Tasnim et al. [3] .As can be seen from the table 2; very good agreements exist between the results of the current simulation and those of Tasnim et al. [3].

Table 2 Comparison of the average Nusselt number with the published study of Tasnim et al. [3]

Ra	Tasnim et al. [3]	Present results
10^3	3.251	3.268
10^4	3.255	3.257
10^5	3.903	3.900
10^6	9.331	9.325

In addition, for the case of presence of the magnetic field, we test our code with the results of Rudraiah et al. [23] in terms of the average Nusselt numbers for different Hartmann numbers and for Grashof number equal to 2×10^5. The comparison results (See Table 3) show a very similar resemblance.

Table 3 Comparison of the average Nusselt number for various Hartmann numbers.

	Nu_{Avg}	
Ha	Rudraiah et al. [23]	Present study
0	4.919	4.917
10	4.204	4.208
50	2.845	2.844
100	1.432	1.429

In order to determine a proper grid for the numerical simulation, a grid independence study is under taken for mixed convection inside the ventilated L-shaped cubic cavity with Re = 500 and Ha = 100 filled with the Cu-water nanofluid (φ = 5%). With five different uniform grids, namely; 56^3, 60^3, 64^3, 68^3 and 72^3 are employed and for each grid size, average Nusselt number of the hot walls is obtained. Fig. 2 shows the average Nusselt number for different grids size obtained by the current simulation. As it can be observed from this figure, a 68^3 uniform grid is sufficiently finer to ensure a grid independent solution.

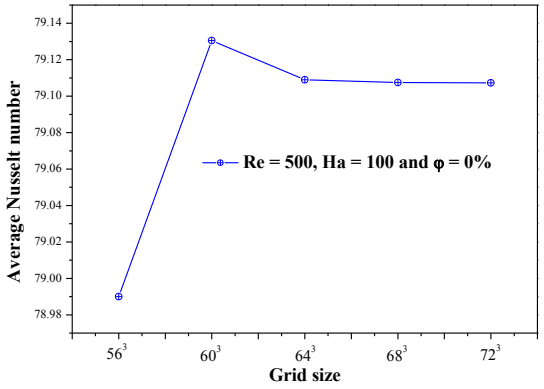

Fig. 2 Effect of the grid size on the Average Nusselt number

RESULTS AND DISCUSSION

In mixed convection within the three-dimensional cavity of 'L' shape, we present the essential results found in functions of the control parameters governing the physical problem, the intensity of the magnetic field (Ha), the Reynolds number (Re) and volume fraction nanoparticles (φ).

The qualitative visualization of the streamtraces and the isotherms distribution in the median plane (X-Y) at Z = 0.50 for the two Reynolds numbers Re = 50 and 500 as a function of the Lorentz force intensity for the case of pure water is illustrated in **Figs. 3** and **4**, respectively. First, in absence of magnetic field we note for lower Reynolds value (Re = 50) that the streamlines distribution is characterized by open lines occupying the majority of the cavity with the presence of small vortex located below the inlet port and rotates in clockwise direction. However, for higher Reynolds number value (Re = 500) we observe the three rotating vortices

Corresponding author: sddikr@yahoo.fr

formation. The first (CW) vortex located below the inlet port, the second (CCW) vortex is located at the right corner near the top wall and the third is found near left vertical wall (X = 0.50) and rotates in clockwise direction. Indeed, in the presence of the magnetic field we clearly see that the recirculation zones disappear completely from the cavity for Re = 50.On the other hand, for Re = 500, the applied vertical magnetic field causes the reduction of the recirculation size zones gradually with the increase of the intensity of the magnetic field.

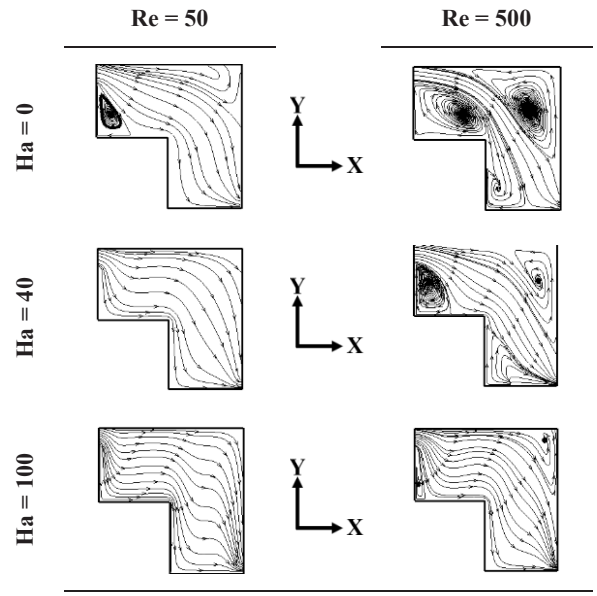

Fig. 3 Streamlines versus Hartmann et Reynolds numbers for pure water at the plane XY (Z = 0.50).

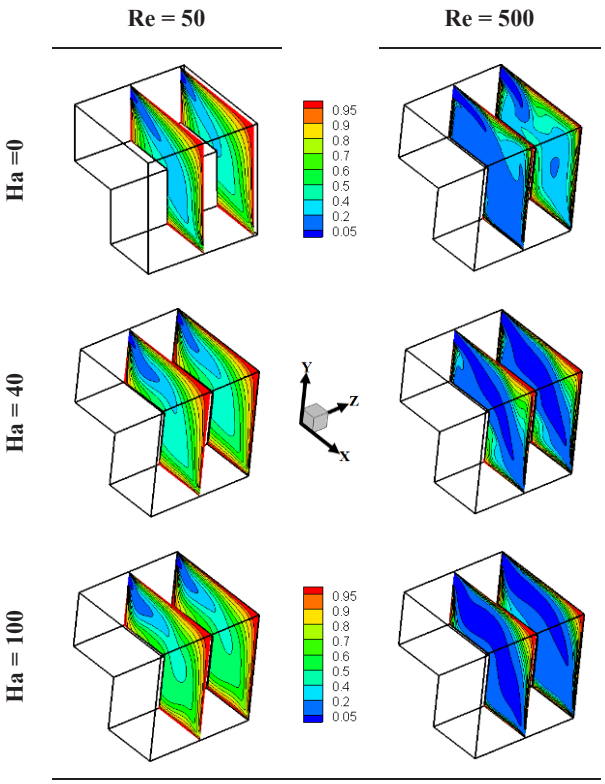

Fig. 4 Hartmann et Reynolds numbers effects on the isotherms for two planes (XY) Z = 0.50 and Z = 0.95 at φ = 0%

Fig. 4 shows the morphology of the isotherms distribution. We find that the effect observed on the streamtraces has repercussions on the isotherms. In the absence of the magnetic field, we notice that the increase in the Reynolds number intensifies the convection currents which are manifested by a distortion of the isotherms. Indeed, in the presence of a magnetic field, we find that the isotherms tend to become parallel to each other near the hot walls as a function of the increase of Ha, thus reflecting a heat transfer by conduction. Thus, the analysis of the thickness of the boundary layer shows through the same figure shows that the boundary layer thickness gradually increases with the increase in the Hartmann number and decreases with increasing Reynolds number. In addition, the study of the adiabatic sidewalls effects, allows us to observe that the isotherms distribution in the two planes XY at Z = 0. 50 and Z = 0.95 are almost identical for Re = 50 and different Hartmann numbers. On the other hand, for Re = 500, the symmetry between the different planes is observed only for the case of the Hartmann number equal to 40. This can be explained by the interaction between the intensity of the descending flow in the part of the cubic cavity. (0.50 ⩽ X ⩽ 1) and the Lorentz force.

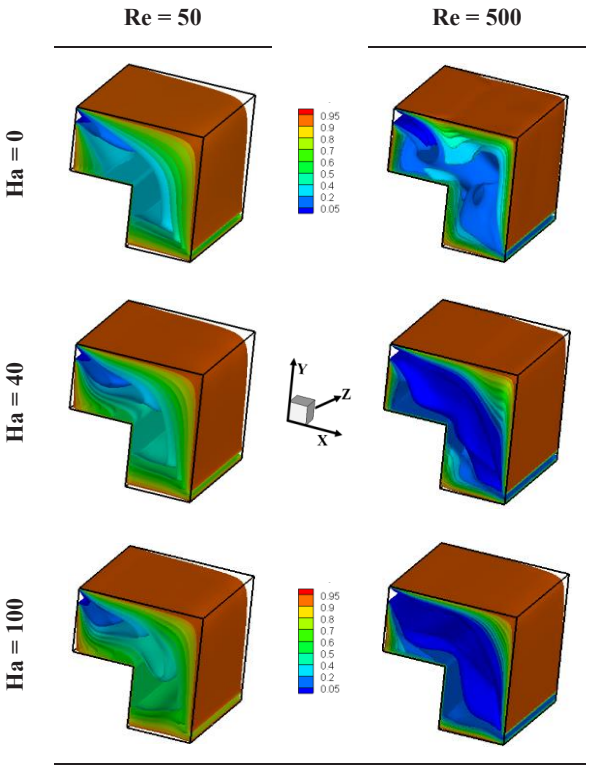

Fig. 5 Temperature isosurfaces for different Reynolds and Hartmann numbers at φ = 0%.

In order to understand the three-dimensional temperature evolution in the third direction OZ, we make in Fig. 5 the temperature isosurfaces distribution with the variation of the Reynolds and Hartmann numbers for the same temperature values (θ) We notice that when the magnetic field is absent (Ha = 0), the isothermal patterns are compressed in a non-uniform fashion indicating that the heat is transferred mainly by convection. Contrary, when Hartmann number is high (Ha = 100) the isothermal lines diverge and take the form of vertical parallel lines indicating

Corresponding author: sddikr@yahoo.fr

that the heat is transferred mainly by conduction, again this effect is due to a slow down of the flux by the magnetic field and especially when the inertia force is low (Re = 50) .In addition, the Reynolds number has a significant influence on the temperature distribution. At low Reynolds number (Re = 50) the isotherms are uniform due to the weak effect of the inertia force with respect to the buoyancy-induced force. But, when the Reynolds number is high (Re = 500), the isotherms are compressed and highly non uniform due to strong inertia forces.

We are interested in the analysis of velocity profiles taking into account the combined effects of Ha and volume fractions in nanoparticles (0 and 5%). Fig. 7 shows the velocity components U for Re = 50 and Re = 500 in the direction OX (Y = 0.75, Z = 0.50). For Re = 50 (Fig. 7a), we notice that the velocity intensity decreases in absence of the magnetic field. This is due to the Lorentz force which is in the opposite direction of the flow (See Momentum equations) .In addition, in the presence of the magnetic field we note that the addition of the nanoparticles increases the velocity only in the part ($0.5 \leqslant X \leqslant 1$) of the cubic cavity due to the increase of the density of descending fluid. But in the presence of the magnetic field, the addition of nanoparticles to the intensity velocity is negligible because the inertia flux has decreased significantly. In the case of Re = 500 (Fig. 7b), as previously the applied of a magnetic field weakens the intensity velocity. Indeed, we observe that the addition of 5% nanoparticles in the absence of the magnetic field reduces the intensity velocity in the first part of the cavity ($0 \leqslant X \leqslant 0.50$), then we attend the increase in velocity in the second part of the cavity ($0.5 \leqslant X \leqslant 1$). This is due to the importance of the main downstream flow. However, in the presence of the magnetic field we notice that the addition of nanoparticles has a negligible effect.

Concerning the vertical velocity component V, we have schematized the isocontours evolution of the velocity V in two planes (X-Z) and the maximum values of the velocity V by the isosurfaces (Green color) in the same figure for two Hartmann numbers (Ha = 0 and Ha = 100) (See Fig. 6b). Through this figure, we notice that the magnitude of the velocity becomes uniform when Ha = 100 compared to the case of the absence of the magnetic field (Ha = 0). This is strongly due to the weakening of the effect of the adiabatic sidewalls. Thus, we find that the maximum velocity for Ha = 100 is located only nears the inlet and the outlet ports of the cavity in comparison with the case of Ha = 0, where the maximum velocity is localized near the vertical right wall.

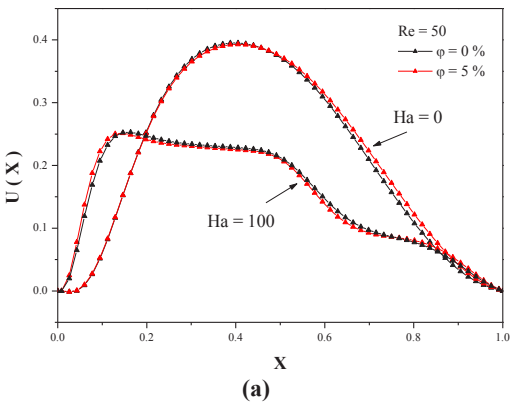

(a)

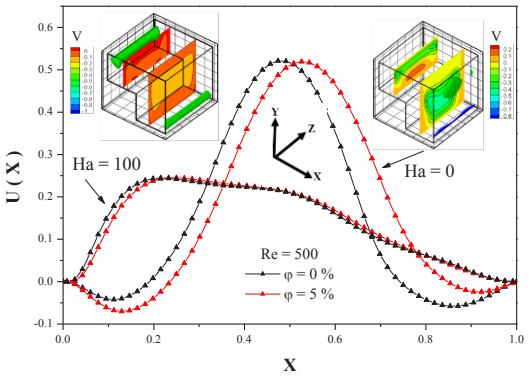

(b)

Fig. 6 U-velocity profiles versus Ha and φ: (**a**) Re = 50, (**b**). Re = 500

The average Nusselt number variations with Hartmann and Reynolds numbers for φ = 0% and φ = 5% are presented in Fig. 7, we clearly see that increasing the incoming flow intensity (Re) the heat exchange rate increases. Indeed, the applied vertical magnetic field has a different impact on the evolution of heat transfer rate with the incoming flow intensity. Indeed, for lower Reynolds number value (Re = 50), we notice that the increase of the Hartmann number makes reduces the average Nusselt number. This can be explained by the fact that in the presence of the magnetic field the total disappearance of the recirculation zones that they are responsible for the heat exchange (walls / flow). On the other hand, for the high value of the Reynolds number (Re = 500), we find that the increase of the magnetic field intensity makes slightly improves the heat transfer rate beyond the value of Hartmann number Ha = 40, then remains almost constant in the interval ($40 \leqslant Ha \leqslant 100$). In addition, we note that the use of nanoparticles have a favorable effect on the heat transfer enhancement. In which, we find that the addition of 5% nanoparticles in the absence of the magnetic field increases the exchange rate beyond 13.12% and 17.74% for Re = 50 and Re = 500, respectively. In the presence of the magnetic field (Ha = 100), we find that the rate improvement is of the order of 13.66% and 18.57% for Re = 50 and Re = 500, respectively. Therefore, the presence effect of the magnetic field has a favorable influence on the improvement of heat transfer. This can be explained by the fact that the addition of nanoparticles is favorable in conduction transfer mode.

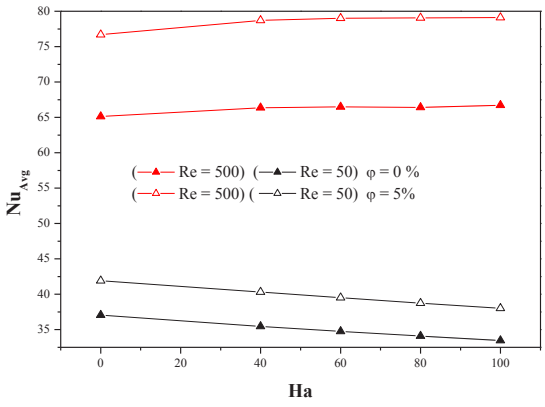

Fig. 7 Ha and Re numbers effects on the average Nusselt for φ = 0% and φ = 5%.

Corresponding author: sddikr@yahoo.fr

CONCLUSION

In the present study, we studied heat transfer within a ventilated L-shaped cubic cavity filled with Cu-water nanofluid under vertical direction of uniform magnetic field. The main results are:

- Increasing the Reynolds number intensifies the hydrodynamic field and improves heat transfer, especially in the absence of the magnetic field.
- The magnetic field weakens the hydrodynamic structure and the convective heat transfer in the cavity for lower Reynolds number value. But, for Re = 500, the magnetic field causes an insignificant improvement of the heat transfer.
- Nanoparticles enhanced the heat transfer performance especially for higher Reynolds number value regardless of the case; the presence or absence of the magnetic field.
- The effect of the third direction is negligible in the presence of the magnetic field.

KEYWORDS: Three-dimensional L-shaped cavity, Mixed convection, Magnetohydrodynamic, Nanofluids.

REFERENCES

[1] S. Ostrach, 1988, Natural convection in enclosure, ASME J. Heat Transfer 110.

[2] S. Mahmud, 2002, Free convection inside an L-shaped enclosure, Int. Commun in Heat Mass Transf. 29, 1005-1013.

[3] S.H. Tasnim, S. Mahmud, 2006, Laminar free convection inside an inclined L-shaped enclosure, Int, Commun, Heat Mass Transf. 33, 936-942.

[4] S. Mahmud, S. H. Tasnim, Free convection in a cavity with two straight and two arced walls, Int. Commun. Heat Mass Transf. 31 (2004) 525-536.

[5] A. Koka, H. F. Ozotop, Y. Varol, 2008, Numerical analysis of natural convection in shed roofs with eave of buildings for cold climates, Comput. Math. Appl. 56, 3165-3174.

[6] M Sheikholeslami, A. J. Chamkha, 2016, Flow and convective heat transfer of ferro-nanofluid in a double-sides lid-driven cavity with a wavy wall in the presence of a variable magnetic field, Numer. Heat Transfer, Part A 69 (10), 1186-1200.

[7] R. Nasrin, M. A. Alim and A. J. Chamkha, 2012, Combined convection flow in triangular wavy chamber filled with water-CuO nanofluid: Effect of viscosity models, Int. Commun in Heat Mass Transfer 39, 1226-1236.

[8] M. Sheikholeslami, 2015, Effect of uniform suction on nanofluid flow and heat transfer over a cylinder, J Braz. Soc. Mech. Sci. Eng, 37, 1623-1633.

[9] A. .J. Chamkha and E. Abu-Nada, 2012, Mixed convection flow in single and double lid-driven square cavities filled with water-AL2O3 nanofluid: effect of viscosity models, European Journal of Mechanics – B/ Fluids, 36, 82-96.

[10] N. Ben Cheikh, A. J. Chamkha, B. Ben Beya and T. Lili, 2013, Natural convection of water-based nanofluids in a square enclosure with non-uniform heating of the bottom wall, Journal of Modem Physics, 4,147-159.

[11] A. J. Chamkha and M. A. Ismael,2013, Conjugate heat transfer in a porous cavity filled with nanofluids and heated by triangular thick wall, Int. J of Thermal Sciences, 67, 135-151.

[12] R. Nasrin, A. J. Chamkha and M. A. Alim, 2014, Modeling of mixed convection heat transfer utilizing nanofluid in a double lid-driven chamber with internal heat generation, Int. J for Numerical Methods in Heat and Fluid Flow, 24, 36-57.

[13] A. J. Chamkha and M. A. Ismael, 2014, Natural convection in differentially heated partially porous layered cavities filled with a nanofluid, Numer. Heat Transfer, Part A, 65, 1089-1113.

[14] S. Parvin and A. J. Chamkha, 2014, An analysis of free convection flow, heat transfer and entropy generation in an odd-shaped cavity with nanofluid, Int. Commun in Heat and Mass Transfer, 54,8-9.

[15] B. Ghasemi, S.M. Aminossadati, A. Raisi, 2011, Magnetic field effect on natural convection in a nanofluid-filled square enclosure, Int. J. Therm. Sci, 50 (9), 1748-1756.

[16] A.H. Mahmoudi, I. Pop, M. Shahi, 2012, Effect of magnetic field on natural convection in a triangular enclosure filled with nanofluid, Int. J. Therm. Sci. 59, 126-140.

[17] B. Ghasemi, 2013, Magnetohydrodynamic natural convection of nanofluids in U-shaped enclosures, Numer. Heat Transfer, Part A, 63, 473-487.

[18] Hillal M. Elshehabey, F.M. Hady, Sameh E. Ahmed, R.A. Mohamed, Numerical investigation for natural convection of a nanofluid in an inclined L-shaped cavity in the presence of an inclined magnetic field, Int. Commun Heat and Mass Transfer 57 (2014) 228-238.

[19] Mohsen Sheikholeslami, Houman B. Rokni, 2017, Simulation of nanofluid heat transfer in presence of magnetic field: A review, Int. Journal of Heat and Mass Transfer, 115, 1203-1233.

[20] H.C. Brinkman, 1952, The viscosity of concentrated suspensions and solution, J. Chem. Phys, 20, 571-581.

[21] J.C. Maxwell, 1873, A Treatise on Electricity and Magnetism, vol. II, Oxford University Press Cambridge, UK, 54.

[22] S.V. Patankar, 1980, Numerical heat transfer and fluid flow, Hemisphere Publishing Corporating, Taylor and Francis Group, New York.

[23] N. Rudraiah, R.M. Barron, M. Venkatachalappa, C.K. Subbaraya, 1995, Effect of a magnetic field on free convection in a rectangular enclosure, Int. J. Eng. Sci, 33,1075-1084.

Corresponding author: sddikr@yahoo.fr